

This work was written as part of one of the author's official duties as an Employee of the United States Government and is therefore a work of the United States Government. In accordance with 17 U.S.C. 105, no copyright protection is available for such works under U.S. Law.

Public Domain Mark 1.0

<https://creativecommons.org/publicdomain/mark/1.0/>

Access to this work was provided by the University of Maryland, Baltimore County (UMBC) ScholarWorks@UMBC digital repository on the Maryland Shared Open Access (MD-SOAR) platform.

Please provide feedback

Please support the ScholarWorks@UMBC repository by emailing scholarworks-group@umbc.edu and telling us what having access to this work means to you and why it's important to you. Thank you.

Prairie Grassland Bidirectional Reflectances Measured by Different Instruments at the FIFE Site

D. W. DEERING, E. M. MIDDLETON, AND J. R. IRONS

NASA Goddard Space Flight Center, Greenbelt, Maryland

B. L. BLAD, E. A. WALTER-SHEA, AND C. J. HAYS

Department of Agricultural Meteorology, University of Nebraska, Lincoln

C. WALTHALL

Department of Geography, University of Maryland, College Park

T. F. ECK, S. P. AHMAD, AND B. P. BANERJEE

Hughes/STX Corporation, Lanham, Maryland

Land surface reflectance measurements were acquired during the First ISLSCP Field Experiment (FIFE) field campaigns using a variety of ground-based and airborne spectral radiometers. To examine the validity of the assumption that the values acquired by the several different instruments and teams were interchangeable, the surface radiation measurement teams converged on a common site for 1 day during the fifth intensive field campaign (IFC 5) in 1989. The instruments compared for near-surface measurements included two ground-based Spectron Engineering SE590s, one helicopter-mounted SE590, one ground-based and one helicopter-mounted Barnes modular multiband radiometer (MMR), and the portable apparatus for rapid acquisitions of bidirectional observations of land and atmosphere (PARABOLA) field radiometer. Comparisons were made for nadir measurements over a range of solar zenith angles and a range of off-nadir viewing angles. The bidirectional reflectances from the different instruments were generally found to be quite comparable. For example, for a 52° solar zenith angle, the nadir red and near-infrared spectral reflectance factors ranged from 3.5 to 4.5% and 28.2 to 31.9%, respectively. At the smaller solar zenith angles, however, the differences were somewhat greater (red, 4.5–6.1%; near-infrared (NIR), 25.0–28.9%), and the coefficients of variation for the samples taken by all of the instruments increased. Off-nadir viewing caused major departures from nadir bidirectional reflectances (30% reflectance at nadir compared with 55% at 60° off nadir in the NIR, for example), but all of the instruments captured the effects reasonably well. Spectral vegetation indices were found to have a considerable dependence on both solar zenith angle and sensor viewing angle. In spite of the general agreement between most instruments and teams, the lack of a more consistent band-to-band agreement resulted in appreciable differences in the spectral vegetation index values, which could potentially affect the accuracy and precision of remote sensing assessments of biophysical parameters.

1. INTRODUCTION

Land surface reflectance measurements, such as those acquired during the First International Satellite Land Surface Climatology Project (ISLSCP) Field Experiment (FIFE) field campaigns in 1987 and 1989 using field and airborne spectral radiometers, provide information about the land surface characteristics, such as albedo, for investigations of surface energy and mass exchanges. This reflectance information is also destined to be used as surrogates for a multiplicity of environmental and biophysical variables, potentially yielding from satellites information such as the amount and condition of the vegetation and estimates of the magnitude of surface fluxes. The FIFE surface radiance data sets had three purposes: (1) to relate the observed radiances with surface biophysical and physical states [Sellers *et al.*, 1990]; (2) to define the spectral and angular components of

the reflected radiation and to compare the surface radiances and reflectances directly to corresponding satellite observations [Sellers and Hall, 1987]; and (3) to use these surface and satellite data sets to test various methods of integrating small-scale processes (for example, photosynthesis, transpiration, scattering of light by leaves) up to the scale of satellite pixels [Sellers *et al.*, 1990].

In general, the scattering phase functions of land surfaces are not isotropic, particularly for vegetation canopies [Deering, 1989]. The knowledge of the reflectance of a surface of interest at several different view and illumination angles may become essential for the extraction of quantitative information about the surface biophysical parameters. Bidirectional reflectance distribution information about a terrestrial surface may be essential when dealing with multisensor and multitemporal data sets containing angular constraints. Accurate and reliable measurements of the surface bidirectional reflectances were needed from the array of radiometers used in FIFE to study the relationships between ground variables and remote sensing measurements and to develop and test

Copyright 1992 by the American Geophysical Union.

Paper number 92JD02163.
0148-0227/92/92JD-02163\$05.00

algorithms for the use of satellite data to estimate these ground variables.

1.1. Rationale

Ideally, measurements would be directly compared from ground to aircraft to satellite, but different instruments were used for these purposes at different sites and times. Thus there is warranted concern about the intercomparability of radiances and reflectances obtained with the different instrument systems. Even the simplest field spectrometers can vary substantially from similar instruments in their design (for example, spectral band pass, electronic characteristics, temperature sensitivities) and use and, consequently, their performance [Deering, 1989]. More sophisticated sensors, such as aircraft instruments, including the advanced solid state array sensor (ASAS) instrument used in FIFE and examined cursorily in this study, have the potential for even more complex variations in sensor response to surface radiance phenomena. For example, Flittner and Slater [1991] have shown that interference filters by different manufacturers can exhibit shifts to higher or lower wavelengths as a result of temperature changes, and aircraft sensors are often subjected to significant changes in ambient temperature, from weather or changes in altitude. Markham and Ahmad [1990] reported that the NS001 multispectral scanner experienced errors of 15–25% owing to problems in internal calibration. Polarization sensitivities were found to cause radiance errors of up to $\pm 10\%$, which vary with scan angle and wavelength.

The need to have accurate instrumentation with high precision in measurement performance is documented by the FIFE study results reported by Hall *et al.* [1991]. For example, surface measurements of reflectance during 1987 showed that during the peak of the growing season on July 11 and August 15 the site-averaged green leaf area index changed by a factor of 2 (1.55–0.8), whereas average reflectance in the visible bands changed by only 1–3% and average reflectance in the infrared changed by 4–9%. Because the measurable changes in reflectance appear to be relatively small (within season and spatially averaged over a diverse regional site), as compared to the observed changes in the biophysical parameter of interest in this example, then the accuracies of the surface ground measurements of the at-the-surface remote sensing variables (reflectances, for example) must be high to evaluate the errors in the remote sensing of the biophysical variables. If the reflectances measured by different instruments show differences in reflectance of the order of these benchmark amounts, then serious problems could result from trying to develop parameter relationships and remote sensing retrieval algorithms that might use data from the different instruments.

Slater [1985] reported on the need for accurate radiometric data for the verification and use of scene radiation models and discussed the wide variety of problems associated with obtaining accurate reflectance measurements. He concluded that 1.5% is the lowest uncertainty we can expect to achieve in field reflectance factor measurements and speculated that this high accuracy may be achievable only in the measurement of extended flat surfaces with reflectances greater than 0.3 and for small solar zenith angles and a clear stable atmosphere.

Until very recently, the performance of different spectral

radiometers was seldom compared. Holm *et al.* [1989] compared atmospherically corrected thematic mapper spectral reflectances of cropland targets to those measured using simple ground-based and low-altitude, aircraft-mounted radiometers of the same type. Over a range of 2–55% reflectance their reflectance factors agreed to ± 1 –2% absolute for comparisons made for well-maintained agricultural areas in which the fields were laser leveled and highly uniform in reflectance. Pinter *et al.* [1990] recently compared ground, aircraft, and satellite measurements of the bidirectional reflectance factors for soil, cotton, and wheat fields in Arizona. They found very good agreement with ground- and aircraft-based nadir observations, and although good agreement was found with off-nadir ground and satellite observations, there was a substantial apparent systematic bias. Pinter *et al.* concluded that such instrument intercomparisons are essential for understanding the complex issues involved in realistic remote sensor data acquisitions (multi-scale/view angle/time-of-day/sensor) that are to be used in the quantification of ground parameters.

Knowledge of atmospheric characteristics and spatial variability across the terrain of interest is also important. The total error in high-altitude remote sensing measurements of the surface can be considered as an additive system, where the total variance (σ_T^2) is the sum of variances from various surface sources ($\sigma_1^2 \dots, \sigma_n^2$), atmospheric sources ($\sigma_{11}^2 \dots, \sigma_{1n}^2$), and other sources (σ_m^2), or

$$\sigma_T^2 = (\sigma_1^2 + \sigma_2^2 + \dots + \sigma_n^2)_{\text{Surface}} + (\sigma_{11}^2 + \sigma_{12}^2 + \dots + \sigma_{1n}^2)_{\text{Atmosphere}} + \sigma_m^2 \quad (1)$$

The relative importance of the surface versus the atmospheric components from these platforms is difficult to assess. At the surface, however, on clear days the relative contribution to the total variance associated with the surface factors alone can be evaluated simply as

$$\sigma_T^2 = (\sigma_1^2 + \sigma_2^2 + \dots + \sigma_n^2)_{\text{Surface}} + \sigma_m^2 \quad (2)$$

The sources of variability in the surface nadir measurements include (1) the instrument differences in number of spectral bands (or spectral samples, for “continuous” spectra); (2) the instrument spectral band placement and bandwidth differences; (3) the calibration algorithms and procedures; (4) the illumination conditions, including the time interval required to obtain a complete measurement set and the time of day (changing background effects with either a static or dynamic canopy architecture), which are associated with the mean and/or range in the solar zenith angle per measurement set; (5) the relative spatial displacement (that is, similar sky conditions) and spectral comparability of irradiance data used in the reflectance computations; (6) the ground area or “patch” size sampled (determined by the sensor instantaneous field of view (IFOV) and height above the ground), which is important relative to the spatial heterogeneity of the scene elements of interest across the site; (7) the spatial sampling scheme; and (8) the density (that is, leaf area index (LAI)) of vegetation actually sampled (closely related to the two above factors).

1.2. Objectives

Two ground-based teams from the surface radiation and biology group (SRB) were primarily responsible for acquiring

ing detailed bidirectional reflectance measurements at selected study sites during the five FIFE intensive field campaigns (IFCs), in 1987 and 1989. They were SRB2 (Blad, Norman, and Walter-Shea) and SRB3 (Deering and Middleton), as referred to by *Sellers et al.* [this issue]. These teams are referred to herein as the University of Nebraska (UNL) and NASA Goddard Space Flight Center (GSFC) teams or their instruments, respectively. Measurements made by these two teams provided baseline data for characterizing the surface anisotropy of the FIFE prairie grasslands [Deering and Middleton, 1990; Middleton, this issue] and for interpreting remote sensing observations acquired from helicopter, aircraft, and satellite sensors.

The number of sites within the FIFE region that the surface-based observation teams could measure during one IFC was limited owing to logistical problems and the availability of clear sky conditions. Thus the experimental design called for the low-altitude helicopter-based system to provide rapid sampling of many sites during a 2-hour flight [Walthall and Middleton, this issue] to obtain representative spectral and spatial radiometric measurements that would provide some comparability to the direct surface measurements and a link to the higher-altitude aircraft and satellite sensors.

Since several different spectral radiometers and data acquisition methodologies were utilized at different FIFE sites and on different platforms to complement one another, to increase the available ground coverage, and to provide "ground truth" for comparisons with satellite sensor data, it was important that these independent measurements be compared. Thus the different surface radiation measurement teams attempted to converge on the same site at the same time to acquire surface bidirectional reflectance data to make such a comparison possible. The objective of this paper is to present the results of the comparisons of the multispectral surface radiances and reflectance factors obtained from the laboratory-calibrated ground and aircraft instruments over a common grassland site to determine whether, and to what extent, sources of surface measurement variations yielded differences. Owing to the complexities in such an intercomparison the focus in this paper is on the nadir comparison results with a limited overview of the off-nadir results. The information from these intercomparisons is vital for the interpretation of any observed differences in reflectance on the FIFE site and should also prove valuable for the design of future experiments.

2. METHODS AND INSTRUMENTATION

The date and site chosen for the intercomparisons in this report was August 8, 1989, at site 916 (4439-ECV). The general uniformity of the April-burned prairie grassland at site 916 can be seen as the backdrop of the instrument setups in Figure 1 and in the vertical bird's-eye-view photographs in Figure 2. Mean canopy height was 35 cm, and average green LAI was 2.2 (standard deviation was 0.79).

The data were collected under clear sky conditions for the time period 0942 to 1000 central daylight time (CDT). The measurements made from 1515 to 1530 CDT were acquired with approximately 15% cumulus cloud cover, but the clouds were to the east of the measurement site. The percentage of diffuse irradiance was computed from an integration of the directional sky irradiance measurements

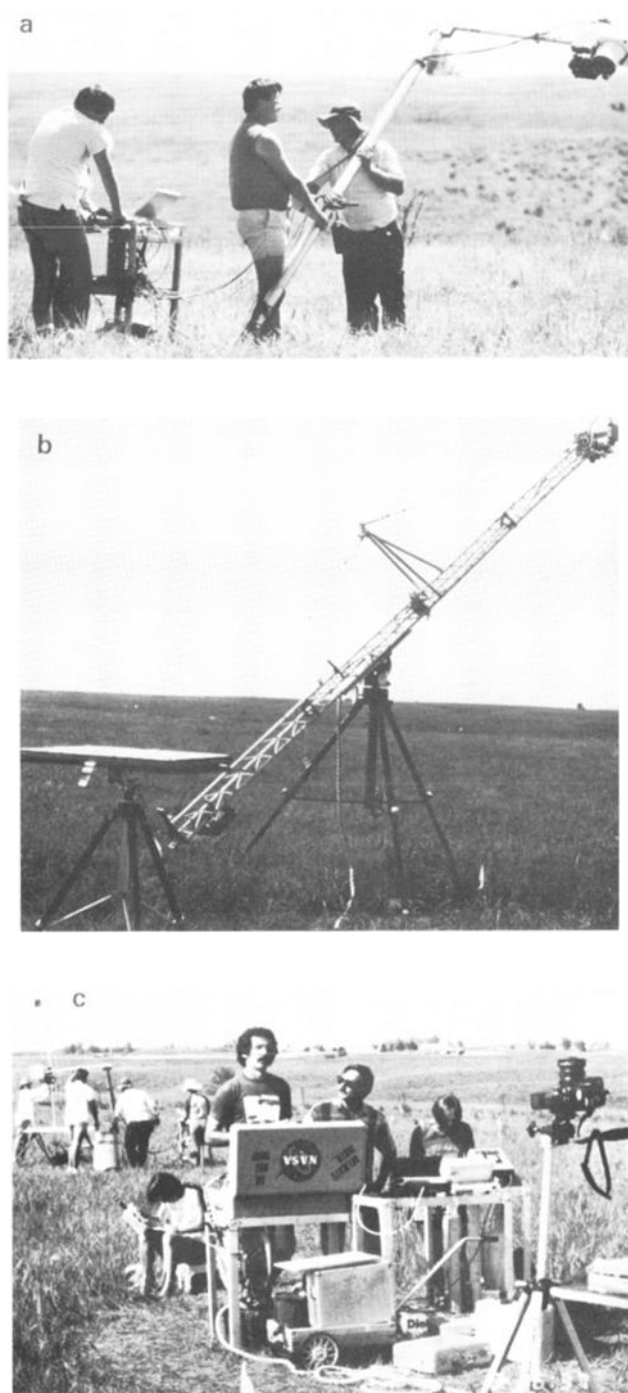


Fig. 1. FIFE site 916 (4439-ECV) prairie grassland and ground instruments: (a) University of Nebraska (UNL) Barnes modular multiband radiometer (MMR) and SE590 in off-nadir viewing mode, (b) portable apparatus for rapid acquisitions of bidirectional observations of land and atmosphere (PARABOLA) multidirectional field radiometer mounted at the end of the triangular truss boom on a 2-m-high tripod, along with the Goddard Space Flight Center (GSFC) SE590, and (c) the data recording systems for both GSFC radiometers and auxiliary systems showing simultaneous data acquisitions with the UNL and reference Barnes MMRs and the sunphotometer in the background.

from the portable apparatus for rapid acquisitions of bidirectional observations of land and atmosphere (PARABOLA) instrument [Ahmad *et al.*, 1987], divided by barium sulfate reference panel measurements corrected for anisotropy

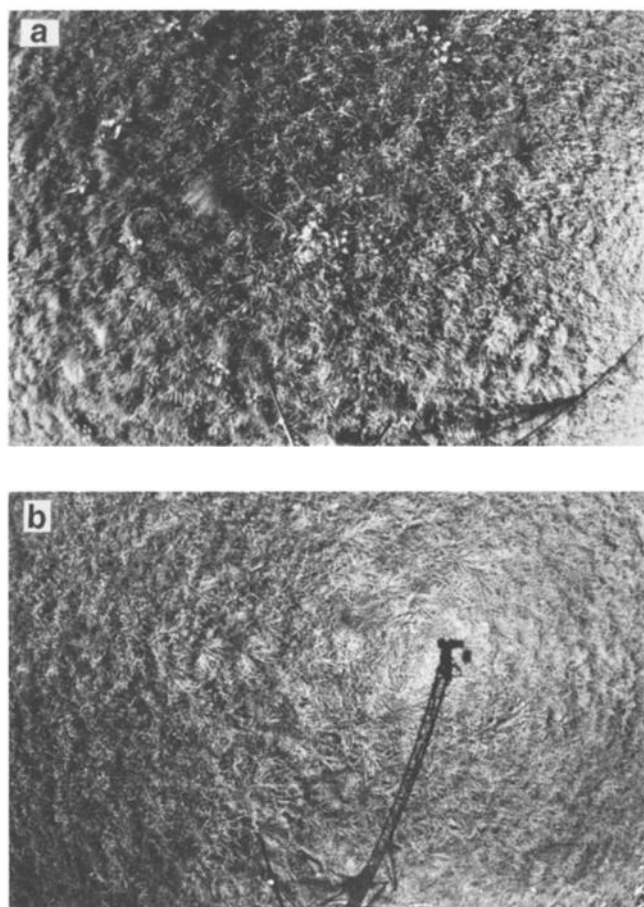


Fig. 2. "Bird's-eye-view" photographs of the site 916 prairie grassland from the PARABOLA system boom head as recorded at (a) 70° and (b) 24° solar zenith angles. The shadow in the image is from the PARABOLA's support boom system and radiometer head. Diagonals are approximately 180° field of view (~130° side to side).

[Jackson *et al.*, 1987]. The percentage diffuse irradiance was greater during the afternoon measurement time period, even though the solar zenith angle was smaller. This additional contribution is believed to be from diffuse flux caused by scattering from cumulus clouds. This is not a large change in the diffuse fraction, however. The diffuse irradiance at 662 nm was 13.8% in the morning with a solar zenith angle (SZA or θ_s) of 50.8° and 18.3% in the afternoon ($\theta_s = 33.5^\circ$). The percentage diffuse irradiance at the 826- and 1658-nm wavelengths were lower at 8.9 and 3.4% for $\theta_s = 50.8^\circ$ and 13.5 and 6.5% for $\theta_s = 33.5^\circ$. The aerosol optical depth, measured with a sunphotometer, also showed increases from morning to afternoon associated with convective processes and the increase in mixed layer depth. The aerosol optical depth at 552 nm increased from 0.14 during the morning period to 0.22 in the afternoon period. At 672 nm the increase was from 0.09 to 0.15; at 872 nm the increase was from 0.06 to 0.10.

The two ground teams (GSFC and UNL) had comparable, though different, instruments, and these two sets of instruments were used in two different data acquisition modes, which are portrayed in Figure 1. The instruments that were compared included two ground-based high spectral resolution SE590s, one helicopter-mounted SE590, one ground-based and one helicopter-mounted eight-band Barnes modular multiband radiometer (MMR), and the ground-based

TABLE 1. Spectral Characteristics of Optical Wave Bands for Instrument Used in the Intercomparison Study

| Instrument* | Channel | Spectral Band Wavelength | | |
|-------------|---------|--------------------------|---------|---------|
| | | Center | Minimum | Maximum |
| SE-590 | na | 485 | 482.5 | 487.5 |
| | na | 560 | 557.5 | 562.5 |
| | na | 670 | 667.5 | 672.5 |
| | na | 820 | 817.5 | 822.5 |
| PARABOLA | 1 | 662 | 641 | 684 |
| | 2 | 826 | 797 | 856 |
| | 3 | 1658 | 1590 | 1730 |
| MMR | 1 | 485 | 450 | 520 |
| | 2 | 555 | 510 | 600 |
| | 3 | 655 | 630 | 680 |
| | 4 | 815 | 750 | 880 |
| | 5 | 1250 | 1170 | 1330 |
| | 6 | 1685 | 1570 | 1800 |
| ASAS* | 7 | 2225 | 2080 | 2370 |
| | 1 | 479 | 471 | 487 |
| | 2 | 563 | 555 | 571 |
| | 3 | 663 | 655 | 681 |
| | 4 | 826 | 818 | 834 |

*The SE590 spectral bands are the integrated wavelength "bands" created for the intercomparisons from the higher-resolution spectral data; na, not applicable. PARABOLA, portable apparatus for rapid acquisitions of bidirectional observations of land and atmosphere; MMR, modular multiband radiometer; ASAS, advanced solid state array sensor (four spectral bands selected from 30).

PARABOLA multidirectional radiometer. The ASAS aircraft system was also included in the comparison for one sampling period. A summary of the instruments used in the intercomparisons described in this paper are given in Table 1.

The two ground teams sampled different, adjacent subsites on FIFE site 916. Instrument intercomparisons were made for nadir measurements conducted in the morning and the afternoon, each at different solar zenith angles. Comparisons were also made for a range of off-nadir viewing angles (θ_v), which depended on the specific sensor and instrument mount characteristics. The data sets selected for the intercomparison study were acquired nominally at a 52° θ_s in the morning and at a 34° θ_s in the afternoon, as given in Table 2.

All instruments were calibrated prior to the experiment, using the GSFC's 1.8-m-diameter integrating sphere, which is equipped with twelve 200-W tungsten filament lamps mounted on the inside of the sphere, and is traceable to the National Institute of Standards and Technology (NIST)

TABLE 2. Surface Radiometry Data Sets Used in the Intercomparisons Study for FIFE Site 916 on August 8, 1989

| Sensor Designation | Team* | Morning Mean θ_s | Afternoon Mean θ_s | Number of Samples |
|--------------------|-------|-------------------------|---------------------------|-------------------|
| G-SE590 | GSFC | 51.9 + 1.0 | 34.0 + 0.25 | 6 |
| N-SE590 | UNL | 51.4 ± 2.5 | 33.8 ± 2.5 | 21–25 |
| H-SE590 | HELO | 54.3 + 0.3 | 33.3 + 1.0 | ≈50 |
| PARABOLA | GSFC | 50.0 + 0.5 | 33.0 + 0.5 | 6 |
| N-MMR | UNL | 51.3 ± 2.5 | 33.8 ± 2.5 | 21–25 |
| H-MMR | HELO | 54.3 + 0.3 | 33.3 + 1.0 | ≈50 |
| ASAS | ASAS | 55.0 | n/a | ≈70 |

*GSFC, Goddard Space Flight Center; UNL, University of Nebraska, Lincoln; HELO, Helicopter.

standard source [Guenther, 1987]. All of the ground-based instruments were fitted with 15° IFOV optics, whereas the helicopter-mounted instruments were fitted with 1° IFOV optics.

2.1. Instrument Descriptions

SE590s. Spectral measurements were obtained with SE590 instruments (Spectron Engineering, Denver, Colorado) operated by the GSFC and UNL ground teams and the helicopter team (referred to as G-SE590, N-SE590, and H-SE590, respectively). The SE590s are continuous spectrum spectroradiometers with wavelengths that span the visible and near-infrared from 400 to 1010 nm with an effective spectral resolution of 10–15 nm, which was resampled at a constant 5 nm. A complete data scan was acquired in approximately 1 s, with an additional 8 s to record the data.

MMRs. Barnes MMRs were used by the UNL ground team, on board the helicopter, and at the calibration site. The MMR is an eight-band (400–2500 nm) commercial radiometer with nominal spectral band centers and band minima and maxima, as shown in Table 1 [Robinson *et al.*, 1979, 1981]. The MMR thermal channel data are not included in this study.

The UNL Barnes MMR (serial number 114) is referred to as N-MMR. The helicopter's Barnes MMR system (serial number 117) is referred to as H-MMR and is described by Walthall and Middleton [this issue]. The H-MMR was the primary helicopter-borne instrument and was considered to be one of the most stable, reliable MMR devices used during FIFE [Markham *et al.*, 1988]. The calibration site MMR (serial number 102) is referred to as R-MMR and was used as the source for irradiances used in the helicopter MMR reflectance factor computations.

PARABOLA. The PARABOLA instrument [Deering and Leone, 1986] is a two-axis scanning head three-channel (visible, near infrared, and midinfrared; 650–670, 810–840, and 1620–1690 nm, respectively), motor-driven radiometer that permits acquisition of radiance data for almost the complete (4π) sky- and ground-looking hemispheres in 15° sectors in 11 s. The radiometer head is mounted together with a nadir-looking camera, which has a wide field of view (16 mm) lens to document the target as observed by the radiometer.

A two-axis leveling mechanism enables accurate orientation of the radiometer head relative to the horizontal. Overall errors in the acquisition of θ_v are estimated to be $\pm 0.5^\circ$ owing to wind and other factors. The measurements acquired from the rapid multiangular sampling by the PARABOLA provide estimates of the bidirectional reflectance distribution function (BRDF), since 264 directional measurements or different off-nadir views are acquired for each of the three spectral bands during each scan.

ASAS. The ASAS airborne sensor acquires digital image data in a push broom fashion for 29 spectral bands covering the range of 468 to 873 nm, with a resolution of 15 nm. At an altitude of 5000 m the sensor's swath width is 2200 m (25° spanned by 512 pixels), and the spatial resolution is 4 m across track and 2 m along track. The accuracy of alignment in any azimuth plane, including the solar principal plane (SPP), is estimated to be $\pm 5^\circ$ – 10° . A gimbaled mounting bracket allows ASAS to be pointed up to 45° off nadir either fore or aft of the platform aircraft [Irons *et al.*, 1991].

Target areas such as FIFE site 916 are located by a visual inspection of the digital image data. The mean and standard deviation of the spectral radiance values within the delineated area are then calculated and stored. ASAS data extracted in this manner from the digital images are at-aperture spectral radiance values that are derived from preflight laboratory radiometric calibration. The ASAS data used in this intercomparison study are atmospherically corrected ground reflectances.

2.2. Bidirectional Reflectance Factors

PARABOLA and G-SE590 bidirectional reflectance factors were computed as the ratio (expressed as a percentage) of the average surface radiance at nadir ($\phi_v = 0$) to the estimated average total irradiance in a particular band. The total irradiance was measured by the GSFC team at each θ_s data acquisition, and reflectance factors were calculated from nadir view irradiances that had been corrected for reflectance anisotropy of the GSFC reference panel (the reflectance standards used are described below), which was located at site 916. The N-SE590 was also placed over a large (1.2 m²) reflectance standard panel at site 916, and reference measurements were acquired every 20–30 min during the intercomparison study. Bidirectional reflectance factors for the UNL and helicopter (HELO) were calculated as the ratio of the averaged upwelling spectral radiance per sensor/band to the best time-based linear estimate of total irradiance available for the appropriate sensor/band, using an anisotropically corrected panel. The helicopter-acquired bidirectional reflectance factors were calculated as the ratio of surface radiances and a 5-min running average of the surface-acquired reference panel radiances (corrected for anisotropy), which were screened for cloud influences and were closely matched to the acquisition times [Walthall and Middleton, this issue].

The ASAS team did not use reference panel measurements. Surface bidirectional reflectance factors were derived from ASAS at-sensor spectral radiance values using a revised version of the simulation of the satellite signal in the solar spectrum (5S) atmospheric radiative transfer code [Tanre *et al.*, 1990]. The 5S code was originally designed to calculate upwelling, top-of-the-atmosphere, bidirectional radiance values on the basis of ground reflectance, atmospheric conditions, and the geometry of illumination and observation. The radiative transfer problem was inverted for this study to derive ground reflectance factors given the upwelling radiance at the altitude of ASAS. The characteristics of a standard atmosphere, U.S. standard 62 [McClatchey *et al.*, 1971], and a continental model of the aerosol distribution were used for the radiative transfer calculations. The measured aerosol optical thickness for 550 nm at the time of data acquisition (0.199) was also input to the 5S code.

Reflectance standard measurements. The GSFC team measured downwelling radiances as the reflected radiation from an unshaded, painted barium sulfate panel maintained in a horizontal position. The panel had been characterized for anisotropic properties by measuring the changes in reflected radiance of the panel (for all of the spectral bands examined in the study) as a function of illumination angle [Jackson *et al.*, 1987]. From these measurements, coefficients were computed to correct the reflected radiances acquired during the field campaigns to provide an estimate of

TABLE 3. A Comparison of Instrument and Sample Site Characteristics for Various Teams in the Intercomparison Study at the 1989 FIFE Site 916

| Instrument or Site Characteristic | Aircraft | | | | | | |
|-----------------------------------|----------|---------|-------|---------|---------|---------|---------|
| | GSFC | | UNL | | HELO | | C-130 |
| | PARABOLA | G-SE590 | N-MMR | N-SE590 | H-MMR | H-SE590 | ASAS |
| Number wave bands | 3 | ~200 | 7 | ~200 | 7 | ~200 | 30 |
| Instantaneous field of view | 15° | 15° | 15° | 15° | 1° | 1° | ~0.05° |
| Diameter at nadir, m | 1.3 | 1.3 | 0.8 | 0.8 | 5.8 | 5.8 | 5 × 2 |
| Reference instrument | PARABOLA | G-SE590 | R-MMR | R-SE590 | R-MMR | R-SE590 | R-SE590 |
| Sample site area, m ² | 100 | 100 | 150 | 150 | 200 | 200 | ~300 |
| Subsite | 1 | 1 | 2 | 2 | 1 and 2 | 1 and 2 | 1 and 2 |
| Number of sets/day | ~15–20 | 9 | 4–5 | 4–5 | 2 | 2 | 2 |

irradiance. The GSFC team had exclusive use of the reference panel at their subsite, from which reference radiances were measured at the beginning and end of each θ_s sampling period by the same instrument used in the measurement of the grassland target (that is, PARABOLA and G-SE590).

A Spectralon panel (Labsphere Incorporated, North Sutton, New Hampshire) was assigned to a fixed calibration site centrally located within the larger site 916 area, and reference data were automatically recorded at 1-min intervals during sampling periods. The reference MMR (R-MMR, serial number 111) was dedicated to the acquisition of reflectance standard panel data. The downwelling radiances were automatically and continuously recorded each field day, beginning 30 min prior to each mission and ending 30 min after the last helicopter mission. These reference data were utilized by the helicopter team to compute reflectances by matching the time in the data records for target and reference scans. However, like the GSFC team, the UNL team used the same instruments for both the upwelling target radiances and the downwelling radiance sampled from the reference panel to eliminate sensor bias effects in the calculation of reflectances. UNL reference measurements were acquired over the Spectralon panel at approximately 30-min intervals [Blad *et al.*, 1990].

The bidirectional reflectances or bidirectional reflectance factors used in this paper can be considered approximately analogous to the hemispherical-conical reflectance factors given by Nicodemus *et al.* [1977]. Slater [1985] considers that it is correct to use “conical” in place of “directional” when referring to measurements made with instruments having 1°–5° IFOVs, like most field radiometers. However, for most aircraft (ASAS, for example) and spacecraft sensors the term directional (that is, hemispherical-directional) is a sufficiently accurate geometrical description. In this paper the terms bidirectional reflectance or reflectance will be the generalized nomenclature used to refer to the appropriate (depending on instrument) radiometric terms.

2.3. Measurement Methods and Sources of Variation

The difference in the measurement acquisition methodology used by the different teams are described in this section, and the characteristics of the team-specific instruments and their related sampling attributes are summarized in Table 3. The nadir view grassland surface measurements reported herein were made as a part of a more comprehensive BRDF characterization activity. These data sets were acquired such that the instruments obtained multiple views at differ-

ent angular positions along the solar principal plane, where $\phi_v = \phi_s$ (ϕ = azimuth). Since the SPP diurnally rotates in azimuth, the instruments were correspondingly rotated to follow the Sun, which often resulted in different grassland patches being sampled within each subsite at different times of day.

The GSFC and UNL ground teams partitioned site 916 into two adjacent subsites within an area of visually uniform prairie cover type (that is, grass/forb mixtures) and plant density to maintain large enough sampling areas to accommodate the diurnal rotation of instruments in the solar principal plane, to allow for trampling disturbances, and to prevent “contamination” of other team instrument-viewing areas. The GSFC boom/tripod support system instruments were placed approximately 5 m above the ground, such that nadir “pixels” were 1.3 m in diameter when viewed with the 15° IFOV. The UNL instruments were closer at 3.4 m above the ground, with nadir pixels of 0.8 m in size. Using these configurations, the GSFC and UNL instruments measured ground areas in the nadir view of 1.35 and 0.52 m², respectively. Since the instruments of each team sampled different-sized patches within their respective grassland subsites, some reflectance differences for the nadir observations may arise owing to sampling differences associated with the variability of the surface cover itself.

For comparisons of ground and airborne instruments the areas measured by the airborne sensors are often larger than those seen by ground instruments and must be adequately characterized by the ground sensors. Thus “one-patch” measurements should be replicated across the larger area represented by the airborne sensor’s IFOV area to account for the variability within that IFOV (that is, subpixels). Failure to adequately replicate and statistically represent the area viewed by the aircraft sensor may result in differences in the ground-based and airborne sensor reflectance measurements.

GSFC. During the FIFE campaigns, the PARABOLA system and the G-SE590 were deployed using a 6.5-m triangular truss boom [Deering and Leone, 1986] on a large tripod (Figure 1b). The G-SE590 was attached to the motorized leveling device of the PARABOLA’s radiometer head mount. With 15° IFOV optics and an offset of only 10 cm the G-SE590 and PARABOLA sampled essentially identical surface areas.

A replicate sampling procedure was used (involving rotation of the boom on the tripod axis at +7.5° and –7.5° on either side of $\phi_v = 0$) with attendant data processing

procedures to increase the spatial sampling and accuracy of the BRDF estimates [Ahmad and Deering, this issue]. Additionally, subsite sample replication was accomplished at several time periods by physically moving the instrument boom system within a few meters of the "home" location; the distance being restricted by the 30-m-long "umbilical" of the data system cabling. Under clear sky conditions the PARABOLA's complete set of angular measurements as well as the G-SE590 nadir measurements were generally acquired at 5° incremental changes of solar zenith angle (θ_s), beginning at approximately 70° or 75° θ_s , to capture the BRDF diurnal dynamics. The subset of these more comprehensive data sets that are examined in this paper were selected to be coincident with the helicopter and ASAS overflights. Figure 3 illustrates that the diurnal dynamics of the nadir view reflectances ($\theta_v = 0$) for site 916 are considerably smaller and less complex than those at the off-nadir angles.

G-SE590 off-nadir measurements in the SPP were generally acquired periodically during a 5- to 10-min time interval. The complete off-nadir sets consisted of observations at 10° ($\pm 0.5^\circ$) increments in θ_v in the solar principal plane from backscatter angles of +50° to forward scatter angles of -60°. These different θ_v s were achieved by remote activation of the roll-axis motor on the PARABOLA's leveling mechanism.

UNL. The UNL instruments were mounted on a portable mast that maintained the sensor heads at 3.4 m from the soil surface. Measurements over the grassland plots were made in the SPP from seven different view zenith angles from backscatter angles of +50° to forward scatter angles of -50°. The mast was determined to be at the appropriate angles by viewing an inclinometer attached to the boom.

The UNL team obtained replicate samples by measuring five to seven subplots, with three replicate measurements each (21–25 samples), at several meter intervals along a circular "transect" circumscribing the perimeter of their subsite at site 916, which the helicopter and ASAS also measured. Repeated sampling during the course of a single day using this approach resulted in significant trampling in the vicinity of the subplots and could have substantially affected the aircraft sensor measurements used in the comparison had they been taken randomly or in linear transects across their subsite. The UNL team acquired a series of nadir and off-nadir measurements at each site that was time consuming and labor intensive with the instrumentation being used (see Figure 1a). Approximately 30 min was required to complete a full transect.

Helicopter. The helicopter instruments were mounted on a pointable apparatus on the starboard side of the helicopter. The pointable mount allowed freedom to acquire view zenith angles (θ_v) in view azimuth (ϕ_v) planes that were independent of the heading of the helicopter. Both instruments (H-SE590 and H-MMR) were triggered nearly simultaneously, with the time of each data observation recorded for each device. An audio and video record of data collection was obtained from a video camera and video cassette recorder (VCR) system. One of the audio tracks of the VCR recorded an audible tone generated each time the instruments were triggered, while the other audio track recorded cabin intercom conversations. These dynamic audio-visual records were essential for processing and analyzing the helicopter data for specific sites.

Helicopter data acquisitions were made above the SRB team sampling sites. A minimum of 20 and a maximum of 150 samples were taken over each site, and the data were averaged to obtain a single value in each spectral band for site 916. Data were collected while hovering 330 m above the surface, which resulted in a nadir footprint of approximately 5.8 m in diameter, covering a ground area of 26 m². Unfortunately, owing to an equipment malfunction, the H-MMR data for the morning comparisons were lost. Data from the H-SE590 and the G-SE590 were used in this study to simulate the H-MMR morning data set for comparisons of the altitude and spatial resolution influences.

ASAS. ASAS data were only available for the morning ($\theta_s = 52^\circ$) comparison. Aerial photography acquired during the ASAS mission was used to identify the separate GSFC and UNL subsites, and the corresponding ASAS pixels (73 for the GSFC subsite and 63 for the UNL subsite) were extracted and averaged separately for the bidirectional reflectance intercomparisons. The nadir ASAS data compared herein are differentiated as ASAS-G for the GSFC subsite and ASAS-N for the UNL subsite.

3. RESULTS AND DISCUSSION

The morning and afternoon ($\theta_s = 50^\circ$ – 55° and 33° – 35° , respectively) nadir view bidirectional reflectances acquired by the instruments at the two selected θ_s at site 916 are given in Tables 4 and 5, respectively. The data are presented for spectral bands that generally correspond to each other from the blue through the shortwave infrared. Narrow-band spectral reflectance factors in the blue (485 nm), green (560 nm), red (670 nm), and near-infrared (820 nm) regions were extracted from the continuous spectra of the G-SE590, N-SE590, and H-SE590 according to the band-pass limits given in Table 1. However, since all of the instruments have both a red (approximately 660–670 nm) and a near-infrared (approximately 820–830 nm) spectral band, the following discussion will focus on the comparability of these spectral band radiances and reflectances.

3.1. Prairie Bidirectional Reflectance Characteristics

PARABOLA measurements have previously revealed considerably different angular reflection properties for a wide variety of natural surface types [Deering, 1989; Deering et al., 1990; Deering and Middleton, 1990; Ahmad and Deering, this issue], and the wide field of view vertical photographs of the prairie grassland of site 916 on August 8, 1989 (Figure 2), illustrate the striking differences in the bidirectional reflectance characteristics that occur with changes in solar zenith angle. Particularly notable is the increase in the amount of sunlit bare soil that is visible as the solar zenith angle decreases (that is, the Sun moves higher overhead; Figure 2b). PARABOLA-measured bidirectional reflectances at eleven viewing angles along the SPP and for six solar zenith angles during the morning of August 8, 1989, are presented in Figure 3 for red, near-infrared, and short-wave infrared spectral band passes.

Off-nadir viewing caused major departures from nadir reflectance (e.g., 32% reflectance at nadir compared with 62% at 60° off nadir for 826 nm at 67° θ_s , PARABOLA; Figure 3), but all of the instruments captured the effects reasonably well, as illustrated by the G-SE590. The prairie grassland exhibited a minimum reflectance near the nadir

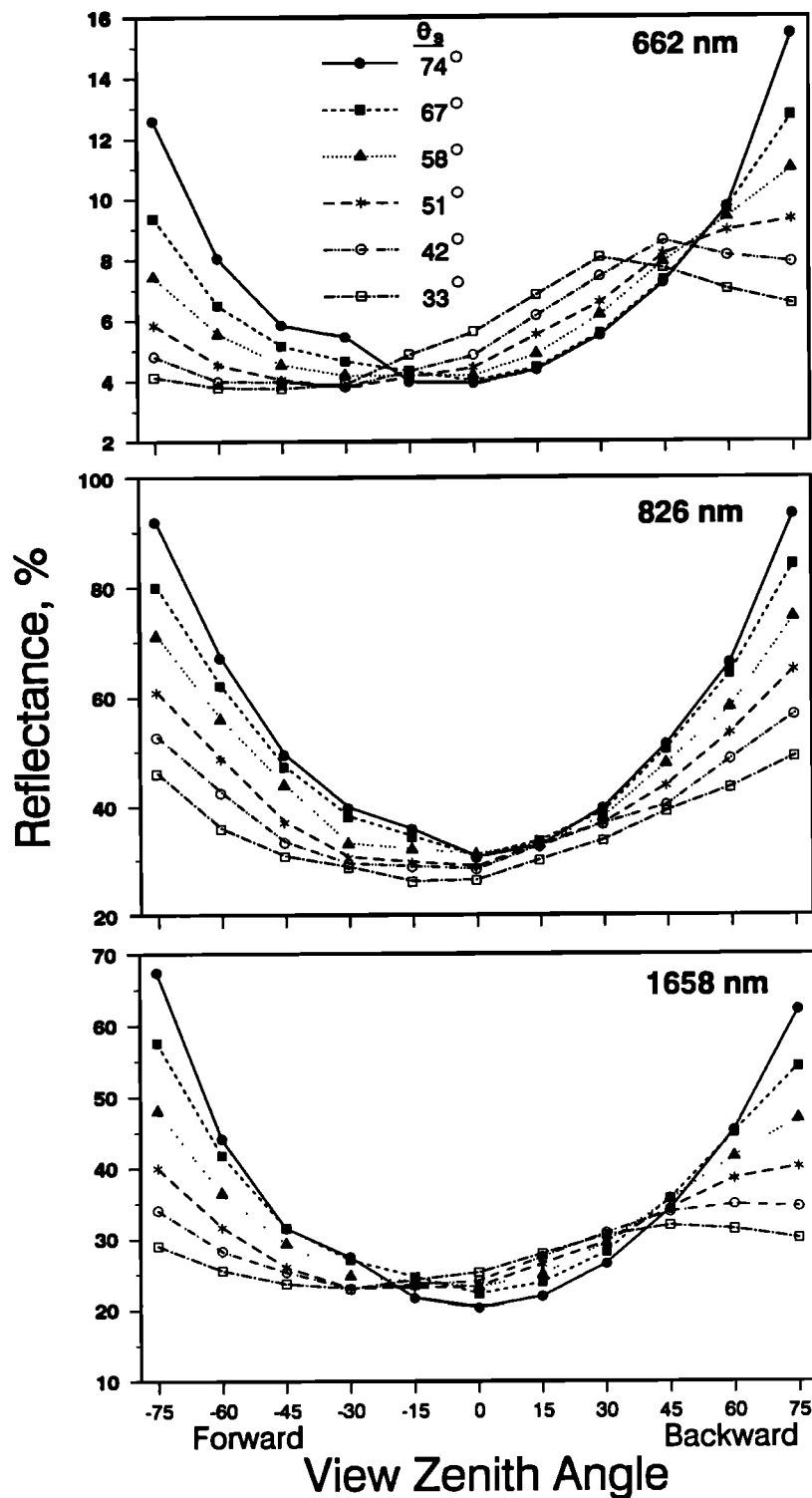


Fig. 3. PARABOLA bidirectional reflectances at nadir and off-nadir viewing angles in the solar principal plane for six solar zenith angles during the morning of August 8, 1989, at FIFE site 916 for spectral wave bands at 662 nm (top), 826 nm (middle), and 1658 nm (bottom).

($\theta_v = 0$) at the larger solar zenith angles, but the minimum shifts toward the forward scatter direction as the Sun moves higher above the horizon, creating a distinctive "hot spot," or no-shadow area, in the region of the antisolar point. This hot spot is particularly pronounced in the red spectral region, is only weakly developed in the shortwave infrared, and is almost

nonexistent in the near-infrared region. The complex light interactions with the plant canopy that are associated with the hot spot phenomenon cause a rise in the bidirectional reflectances at nadir in the more absorptive spectral regions, the red (662 nm) and shortwave infrared (1658 nm) spectral bands, as the solar zenith angle decreases.

TABLE 4a. Nadir Spectral Bidirectional Reflectance Factor Means and Standard Deviations for the 52° Solar Zenith Angle for Selected Wavelength Intercomparisons for Six Instruments at FIFE Site 916

| Wave Band | Statistic | GSFC | | UNL | | HELO/Aircraft | | |
|-----------|-----------|---------|----------|---------|-------|---------------|--------|--------|
| | | G-SE590 | PARABOLA | N-SE590 | N-MMR | H-SE590 | G-ASAS | ASAS-N |
| Blue | Mean* | 3.07 | | 2.70 | 3.38 | 3.55 | 3.80 | 3.60 |
| | s.d. | 0.14 | | 0.12 | 0.12 | 0.19 | 0.20 | 0.30 |
| Green | Mean | 7.00 | | 6.46 | 5.95 | 7.35 | 8.20 | 8.00 |
| | s.d. | 0.18 | | 0.32 | 0.34 | 0.55 | 0.20 | 0.20 |
| Red | Mean | 4.20 | 4.41 | 3.52 | 4.34 | 4.50 | 5.30 | 5.00 |
| | s.d. | 0.26 | 0.21 | 0.24 | 0.27 | 0.24 | 0.20 | 0.40 |
| NIR | Mean | 28.90 | 28.16 | 31.01 | 31.88 | 31.63 | 32.90 | 32.70 |
| | s.d. | 0.74 | 1.04 | 2.61 | 2.74 | 1.45 | 1.20 | 1.50 |
| SWIR 1 | Mean | | | | 33.08 | | | |
| | s.d. | | | | 1.80 | | | |
| SWIR 2 | Mean | | 22.92 | | 18.77 | | | |
| | s.d. | | 0.79 | | 1.08 | | | |
| SWIR 3 | Mean | | | | 9.79 | | | |
| | s.d. | | | | 1.06 | | | |

Original measurements were at a nominal 52° solar zenith angle and were taken during the morning of August 8, 1989; s.d., standard deviation. NIR, near infrared; SWIR, shortwave infrared.

*Expressed in percentage.

In the absence of a significant hot spot effect in the more reflective near-infrared (826 nm) spectral region the nadir bidirectional reflectances decrease as the solar zenith angle decreases. The reflectance increases and decreases at nadir

with changes in solar zenith angle are probably strongly related to the increases in the amount of sunlit bare soil (especially in the red and shortwave infrared) and the decrease in the path length of the radiation through the plant canopy (especially in the near infrared) as the solar zenith angle decreases. Similar "brightness" effects are evident in the backscatter direction viewing off nadir. The G-SE590 reveals a rather consistent, continual increase in reflectance at all wavelengths as the instrument is moved from nadir to the more extreme off-nadir view angles along the SPP (Figure 4a).

A more complex light interaction phenomenon appears to occur in the forward scatter direction. The G-SE590 measurements (Figure 4b) in both the green and the near-infrared spectral regions show first a decline in reflectance as the sensor is pointed at increasingly off-nadir view angles ($\theta_v = 10^\circ$ to 30°) and then an increase in reflectance at the more extreme θ_v (50° and 60°). The red spectral region exhibits a persistent decrease in reflectance at forward scatter off-nadir angles, with a "movement" back toward higher values at the 60° view angle. This unusual feature is remarkably consistent with the PARABOLA red band measurements for the $50.8^\circ \theta_s$ (Figure 3) and was observed in the off-nadir UNL measurements as well.

3.2. Instrument Comparisons at Nadir

In general, the nadir bidirectional reflectance comparisons were good. For example, at a 52° solar zenith angle the nadir red and near-infrared spectral wave band reflectances were very similar, ranging from 3.5 to 4.5% and 28.2 to 31.9%, respectively, for the near-surface sensor measurements (Table 4a). With the Sun at a 34° solar zenith angle there was more variability in the visible wavelengths, and the spread was somewhat greater with reflectances ranging from 4.5 to 6.1% and 25.0 to 28.9%, for red and near-infrared, respectively, for the same instruments. The ASAS measurements for $\theta_s = 52^\circ$ were a maximum of only 1% higher in absolute reflectance for the red band, but in the near infrared, reflectances were more than 4% higher (absolute).

TABLE 4b. Nadir Spectral Bidirectional Reflectance Factor Means and Standard Deviations for Selected Wavelength Intercomparisons for the 52° Solar Zenith Angle With Three SE590 Data Sets Integrated Over ASAS Wave Bands for the Four Other Instruments

| Wave Band | Statistic | GSFC PARABOLA | UNL N-MMR | HELO/Aircraft | |
|--------------|-----------|------------------|--------------|---------------|--------|
| | | | | H-MMR | ASAS-G |
| G-SE590 | | | | | |
| Blue | Mean* | | 3.41 | 3.61 | 3.13 |
| | s.d. | | 0.19 | 0.17 | 0.15 |
| Green | Mean | | 6.15 | 6.15 | 6.56 |
| | s.d. | | 0.22 | 0.22 | 0.19 |
| Red | Mean | 4.52 | 4.77 | 4.77 | 4.53 |
| | s.d. | 0.28 | 0.28 | 0.28 | 0.28 |
| NIR | Mean | 29.03 | 28.94 | 28.94 | 29.28 |
| | s.d. | 0.76 | 0.75 | 0.75 | 0.76 |
| N-SE590 | | | | | |
| Blue | Mean | | 3.19 | 3.51 | 2.83 |
| | s.d. | | 0.25 | 0.18 | 0.13 |
| Green | Mean | | 5.68 | 5.68 | 5.79 |
| | s.d. | | 0.33 | 0.33 | 0.34 |
| Red | Mean | 3.74 | 4.55 | 4.55 | 3.78 |
| | s.d. | 0.25 | 0.31 | 0.31 | 0.25 |
| NIR | Mean | 31.24 | 31.18 | 31.18 | 31.63 |
| | s.d. | 2.73 | 2.67 | 2.67 | 2.68 |
| H-SE590 | | | | | |
| Blue | Mean | | 3.96 | 4.25 | 3.66 |
| | s.d. | | 0.21 | 0.20 | 0.23 |
| Green | Mean | | 6.56 | 6.56 | 6.79 |
| | s.d. | | 0.58 | 0.58 | 0.61 |
| Red | Mean | 4.80 | 5.39 | 5.39 | 4.90 |
| | s.d. | 0.26 | 0.27 | 0.27 | 0.26 |
| NIR | Mean | 31.14 | 31.00 | 31.00 | 31.13 |
| | s.d. | 1.50 | 1.51 | 1.51 | 1.50 |

Original measurements were at a nominal 52° solar zenith angle and were taken during the morning of August 8, 1989.

*Expressed in percentage.

TABLE 5a. Nadir Spectral Bidirectional Reflectance Factor Means and Standard Deviations for the 34° Solar Zenith Angle for Selected Wavelength Intercomparisons for Six Instruments at FIFE Site 916

| Wave Band | Statistic | GSFC | | UNL | | HELO | |
|-----------|-----------|---------|----------|---------|-------|---------|-------|
| | | G-SE590 | PARABOLA | N-SE590 | N-MMR | H-SE590 | H-MMR |
| Blue | Mean | 3.82 | | 3.10 | 3.70 | 3.33 | 4.19 |
| | s.d. | 0.11 | | 0.37 | 0.37 | 0.43 | 0.92 |
| Green | Mean | 6.96 | | 6.00 | 5.90 | 6.75 | 6.47 |
| | s.d. | 0.35 | | 0.32 | 0.25 | 0.26 | 2.71 |
| Red | Mean | 5.60 | 6.13 | 4.47 | 5.23 | 4.59 | 5.61 |
| | s.d. | 0.54 | 0.34 | 0.98 | 0.66 | 0.48 | 2.00 |
| NIR | Mean | 25.49 | 25.32 | 24.96 | 26.85 | 28.18 | 28.9 |
| | s.d. | 0.42 | 0.86 | 3.65 | 3.24 | 1.63 | 0.71 |
| SWIR 1 | Mean | | | | 30.36 | | 34.12 |
| | s.d. | | | | 1.37 | | 4.33 |
| SWIR 2 | Mean | | 24.94 | | 20.62 | | 24.2 |
| | s.d. | | 0.70 | | 1.63 | | 18.68 |
| SWIR 3 | Mean | | | | 13.13 | | 13.17 |
| | s.d. | | | | 2.55 | | 12.35 |

Original measurements were at a nominal 34° solar zenith angle and were taken during the morning of August 8, 1989; s.d., standard deviation.

The coefficient of variation for the samples taken by all instruments was greater at the smaller solar zenith angle. Differences of typically only 1–2% reflectance (absolute) were attributed to the specific band-pass differences of the instruments. A comparison of the reflectances obtained by the

various instruments, normalized to the corresponding reflectances of the unique PARABOLA instrument, reveals that the red band and the near-infrared band values typically differed by only ~1.5% and 4% absolute reflectance, respectively (Table 6). The morning and afternoon comparisons yielded inconsistent results for the same instrument, probably an indication of the degree of precision for our instrument intercomparison.

A direct comparison of the absolute nadir bidirectional reflectance factors (expressed as percent reflectance) indicate general agreement among the three SE590s. The G-SE590 reflectances were between the H-SE590 (higher) and the N-SE590 (lower) reflectances in the visible region (Figure 5). In the near-infrared region the H-SE590 and N-SE590 values are virtually superimposed upon one another and are only slightly higher than the G-SE590. The H-SE590 shows apparent spectral features in the blue and red wavelengths, which are not shown by either identical-model ground instrument. This may point to electronic noise or other problems attendant with use of the helicopter with this instrument. (One of the inverters used to provide power to the helicopter instruments failed several days later. These anomalous spectral features may be due to noise from this device as it began to fail.) Other possibilities are atmospheric effects and reference panel measurement anomalies from using a different instrument for irradiance measurements. The PARABOLA, N-MMR, and H-MMR (actual and simulated from H-SE590) are in good general agreement in both the red and the near infrared.

Reflectances from the two helicopter instruments were generally higher than those of the ground-based instruments of the same type, although some lower values for the H-SE590 were observed in the afternoon relative to the G-SE590. In a comparison of corrected Landsat thematic mapper (TM) at-satellite radiances and helicopter MMR measurements for August 15, 1987, FIFE data, Hall *et al.* [1991] showed good agreement to within 2% in the visible and near-infrared wavelengths and to about 6% in the midinfrared, but the helicopter surface reflectances were consistently higher than the TM-retrieved reflectances. Recent analysis has shown that even at 300 m above ground

TABLE 5b. Nadir Spectral Bidirectional Reflectance Factor Means and Standard Deviations for the 34° Solar Zenith Angle for Selected Wavelength Intercomparisons for Six Instruments at FIFE Site 916 for SE590 Data Integrated Over H-MMR Wave Bands

| Wave Band | Statistic | GSFC PARABOLA | UNL N-MMR | HELO/Aircraft | |
|----------------|-----------|------------------|--------------|---------------|--------|
| | | | | H-MMR | G-ASAS |
| <i>G-SE590</i> | | | | | |
| Blue | Mean | | 4.16 | 4.25 | 3.85 |
| | s.d. | | 0.16 | 0.17 | 0.12 |
| Green | Mean | | 6.38 | 6.56 | 6.73 |
| | s.d. | | 0.38 | 0.39 | 0.35 |
| Red | Mean | 5.75 | 6.00 | 5.39 | 5.78 |
| | s.d. | 0.58 | 0.60 | 0.58 | 0.55 |
| NIR | Mean | 25.53 | 25.36 | 31.00 | 25.71 |
| | s.d. | 0.43 | 0.43 | 0.47 | 0.43 |
| <i>N-SE590</i> | | | | | |
| Blue | Mean | | 3.55 | 3.75 | 3.22 |
| | s.d. | | 0.37 | 0.38 | 0.40 |
| Green | Mean | | 5.52 | 5.52 | 5.62 |
| | s.d. | | 0.31 | 0.31 | 0.35 |
| Red | Mean | 4.59 | 5.26 | 5.26 | 4.62 |
| | s.d. | 1.00 | 0.95 | 0.95 | 0.98 |
| NIR | Mean | 25.13 | 25.11 | 25.11 | 25.45 |
| | s.d. | 3.71 | 3.75 | 3.75 | 3.72 |
| <i>H-SE590</i> | | | | | |
| Blue | Mean | | 3.77 | 3.97 | 3.45 |
| | s.d. | | 0.47 | 0.48 | 0.45 |
| Green | Mean | | 6.13 | 6.13 | 6.32 |
| | s.d. | | 0.25 | 0.25 | 0.27 |
| Red | Mean | 4.79 | 5.32 | 5.32 | 4.83 |
| | s.d. | 0.52 | 0.55 | 0.55 | 0.50 |
| NIR | Mean | 27.67 | 27.59 | 27.59 | 27.58 |
| | s.d. | 1.55 | 1.64 | 1.64 | 1.60 |

Original measurements were at a nominal 34° solar zenith angle and were taken during the morning of August 8, 1989.

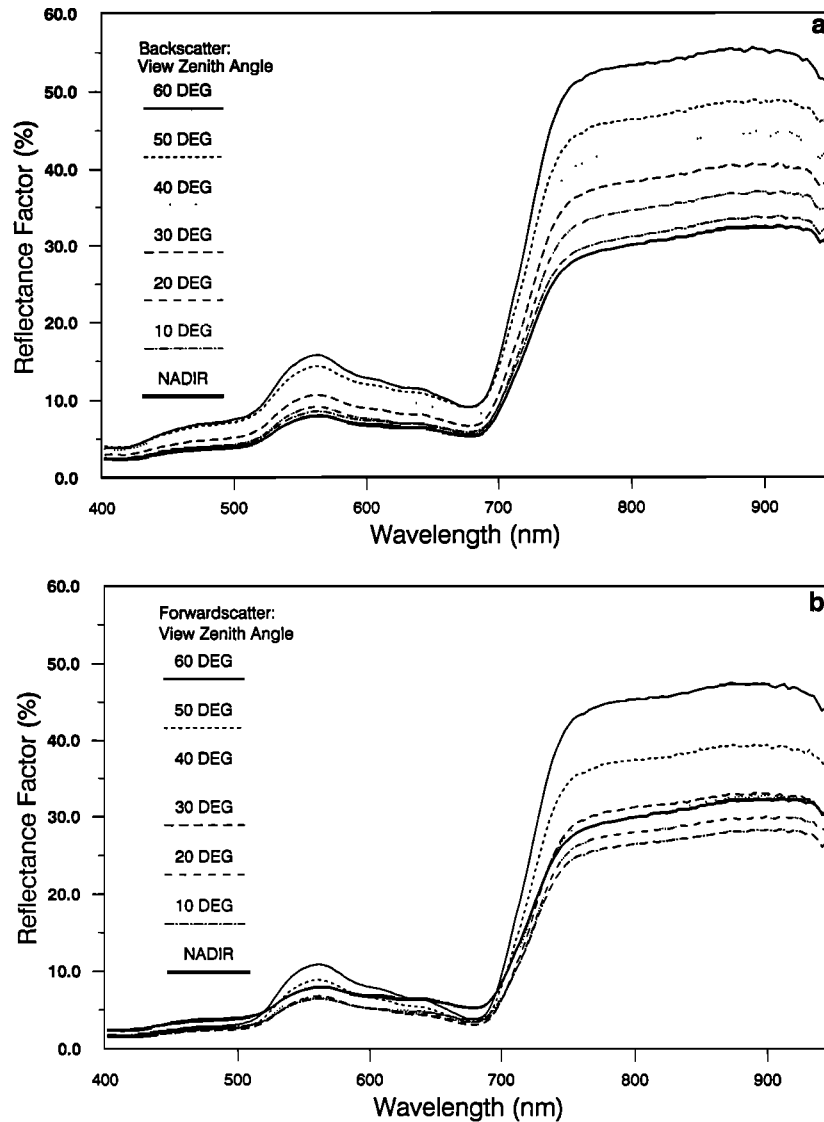


Fig. 4. Spectral reflectance factors at different view angles (θ_v) for the GSFC SE590 at a 53° solar zenith angle in the solar principal plane for (a) backscatter and (b) forward scatter directions.

level (agl) there is sufficient atmospheric path length to reduce differences [Walthall and Middleton, this issue].

Walthall and Middleton [this issue] examined spectral vegetation indices using helicopter MMR data because of the

TABLE 6. Comparisons of Measured and Simulated Nadir Reflectances for Different Instruments Relative to the PARABOLA-Measured Values

| Instrument | 670 nm $\theta_s = 52^\circ (34^\circ)$ | 820 nm $\theta_s = 52^\circ (34^\circ)$ |
|-------------------------|--|--|
| G-SE590 | -0.32 (-0.53) | 0.84 (0.17) |
| N-SE590 | -0.89 (-1.66) | 2.85 (-0.36) |
| H-SE590 | 0.09 (-1.54) | 3.47 (2.86) |
| N-MMR | -0.07 (-0.90) | 3.72 (1.53) |
| H-MMR | (-0.52) | (3.58) |
| ASAS-G | 0.89 (···) | 4.74 (···) |
| ASAS-N | 0.59 (···) | 4.54 (···) |
| <i>Simulated Values</i> | | |
| PARABOLA, from G-SE590 | 1.58 (-0.38) | 2.06 (0.17) |
| H-MMR, from G-SE590 | 0.98 (-0.74) | 2.84 (5.68) |
| H-MMR, from H-SE590 | (-0.13) | (0.04) |

Difference from PARABOLA in absolute reflectance.

widespread use of these indices. They concluded that for a wide range of conditions the simple ratio (SR) appeared to exhibit greater sensitivity to vegetation changes than the normalized difference vegetation index (NDVI). Therefore we examined the SR for nadir measurements at FIFE site 916 computed from radiances and reflectances (Table 7).

The nadir-derived SRs reveal two important features for vegetation index computations. First, the within-group (that is, GSFC instruments, UNL instruments) differences are small. For example, the SR computed from radiance for the G-SE590 and PARABOLA are virtually identical at 4.24 and 4.36 at $52^\circ \theta_s$ and 2.87 and 2.81 at $34^\circ \theta_s$. The comparable UNL values are higher than those of the GSFC instruments, but they are virtually identical at 5.55 and 5.32 at $52^\circ \theta_s$ and 3.72 and 3.72 at $34^\circ \theta_s$. It is conceivable that the GSFC versus UNL differences could be attributable to subsite differences. This hypothesis is supported from the ASAS data, which were extracted separately for the two separate subsites. The GSFC subsite has a lower SR (6.21) than the UNL subsite (6.54), which suggests a correspondingly lower green vegetation cover at the GSFC subsite.

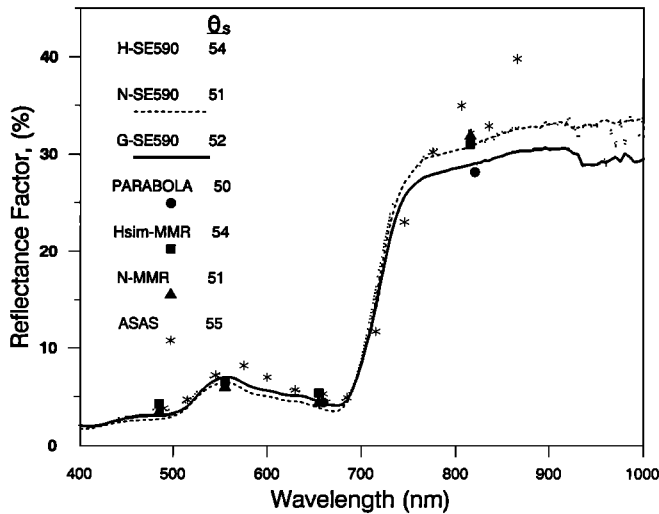


Fig. 5. A comparison of nadir spectral bidirectional reflectance factors for different instruments at a 52° solar zenith angle for the morning of August 8, 1989, at FIFE site 916.

Second, the SR values computed from radiances differ from those computed from reflectances. Therefore it is important to know which method was used when developing or deriving parameter estimates from spectral indices. One impact of these differences is that the choice of instrument could yield different parameter estimates.

Statistical comparisons within and between teams. A more rigorous examination of the agreement between and among the various instrument types and teams was accomplished through statistical *t* tests. Analyses were performed separately for the two solar zenith angles and then by combining the data sets for instruments and teams. Means and standard deviations for each of the instruments are graphically compared in Figure 6a ($\theta_s = 52^\circ$) and Figure 6b ($\theta_s = 34^\circ$). Two of the readily apparent features are the generally larger standard deviations for all instruments at the larger solar zenith angles and the lack of a consistent trend by wavelength bands in reflectance differences for the various instruments.

GSFC: Statistical intercomparisons for the PARABOLA and the G-SE590 can only be performed for the red and the near-infrared regions. The measurements from these two instruments agree, there being no statistically significant differences ($p \leq 0.05$) between the pairs of radiances or reflectances. The absolute differences (PARABOLA minus G-SE590) in radiance ($\text{W m}^{-2} \text{sr}^{-1} \mu\text{m}^{-1}$) in the red band were +0.61 and +1.15 at θ_s of 52° and 34°, respectively. Comparable differences in the near infrared were slightly greater at +2.91 and +1.82. In all cases (2λ , $2 \theta_s$) these differences in grassland surface radiances translated into <1% (absolute) differences in reflectance.

Failure to find a difference between the measurements of these two instruments was not caused by large variability, since the coefficient of variation (CV), expressed as a percentage (% CV), was always <10% for all measurements and was <6% in 14 of the 16 measurement sets. The % CV of the reflectances were almost identical to those for the corresponding radiances, indicating that the irradiances did not contribute additional variation to the measured reflectances. This can be attributed to the method of rapid

self-determination of irradiances by this team under the same sky conditions experienced at the measurement subsite. The 6–10% CV represents the inherent small site variability associated with $\sim 2 \text{ m}^2$ pixels within a visually homogeneous grassland subsite (see Figure 2).

To examine the potential wave band difference influences on the measured reflectances, we simulated the PARABOLA wave bands through a weighted integration of the appropriate G-SE590 high spectral resolution data. Table 6 includes the comparison of these simulated PARABOLA measurements with the actual measurements. Because the two instruments were sampling the “identical” ground patches and reference panel at precisely the same times, the reflectances should be essentially identical. They were almost indistinguishable for the afternoon ($\theta_s = 34^\circ$) data at less than 0.5% absolute reflectance differences. The morning ($\theta_s = 52^\circ$) simulation data differed from the actual PARABOLA reflectances by slightly more than 1.5% absolute, overestimating for both wave bands.

We conclude that the spectral radiances and reflectances acquired nearly simultaneously over virtually the same grassland patch from two very different GSFC instruments exhibited excellent agreement and precision in the two spectral regions and for the two θ_s examined, and the wave band differences were negligible for this grassland surface and under the conditions studied.

UNL: The N-MMR and the N-SE590 are comparable in four spectral regions, the blue, green, red, and near infrared. The N-SE590 consistently measured lower radiances and reflectances in both the red and the near infrared spectral regions, compared with the N-MMR, but all but one of these comparison differences were not statistically significant. The N-SE590 also consistently measured radiances and reflectances that were lower in the blue and higher in the green than the N-MMR, but these differences were statistically significant only for the green band at θ_s of 34° ($0.05 > p > 0.01$).

The mean absolute differences in radiance (N-MMR–N-SE590) in the blue band were 2.48 and 3.44 at θ_s at 52° and 34°, whereas in the green they were –2.26 and –0.96, respectively. The average absolute differences for reflectance in these bands were less than 1%. The mean absolute differences in radiance in the red band were 1.71 and 2.22 at θ_s at 52° and 34°, respectively. Differences in the near infrared were greater at 6.91 and 8.39. Average absolute differences for reflectance were less than 2%.

TABLE 7. A Comparison of Nadir Simple Ratio (SR) Values Computed From Red and Near-Infrared Radiances and Reflectances at Two Solar Zenith Angles

| Instrument | SR From Radiance | | SR From Reflectance | |
|------------|------------------|----------------|---------------------|----------------|
| | 52° θ_s | 34° θ_s | 52° θ_s | 34° θ_s |
| G-SE590 | 4.24 | 2.87 | 7.09 | 4.55 |
| PARABOLA | 4.36 | 2.81 | 6.39 | 4.13 |
| N-SE590 | 5.55 | 3.72 | 8.81 | 5.58 |
| N-MMR | 5.32 | 3.72 | 7.35 | 5.13 |
| H-SE590 | ... | ... | 7.03 | 6.14 |
| H-MMR | ... | 3.69 | 5.75 | 5.15 |
| ASAS-G | 3.06 | ... | 6.21 | ... |
| ASAS-N | 3.14 | ... | 6.54 | ... |

Simple ratio is near infrared/red.

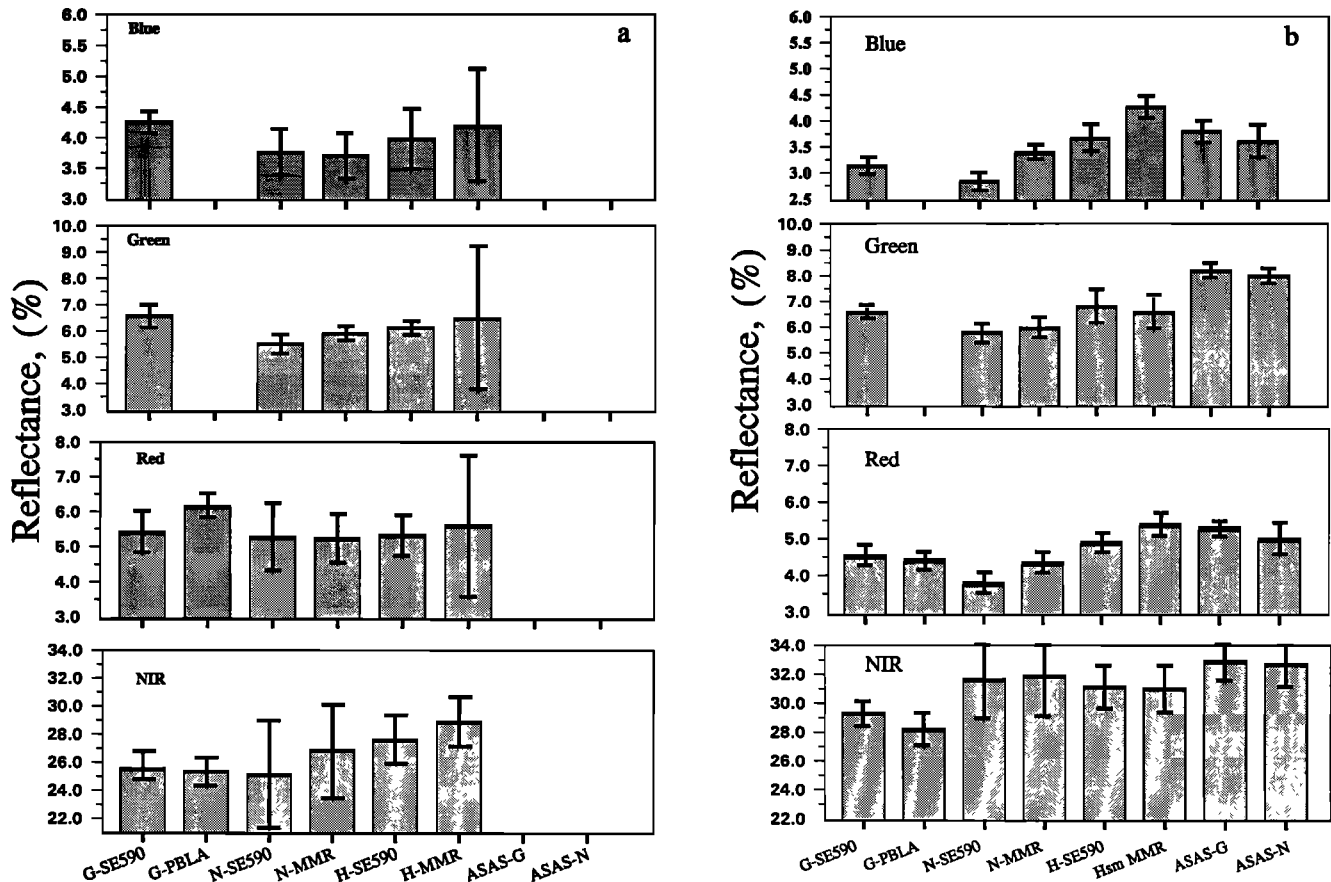


Fig. 6. Nadir reflectances and standard deviations compared for different instruments with SE590 simulations of (a) H-MMR spectral bands and (b) ASAS spectral bands at FIFE site 916, August 8, 1989, $\theta_s = 34^\circ$.

In general, the % CVs for reflectances were similar to those of the corresponding radiances ($\pm 12\%$), indicating that changes in sky conditions over the ground sampling period did not contribute additional variance to reflectance calculations, even though θ_s changed $\approx 5^\circ$ during the acquisition of the BRDF surface data sets. The variation expressed by the % CV for reflectances is attributed to the surface conditions and not to irradiance conditions.

The two instruments used by the UNL team were in good agreement 7 out of 8 times. The % CVs of the measurements indicate the natural variation in the vegetation across the subsite sampled by this team. Discrepancies between measurements of the two instruments may have been caused by a calibration or processing bias not previously realized or different responses due to the wave band interval differences.

GSFC versus UNL: The spectral means obtained from each of the two instruments per team were computed to produce a "subsite" value for radiances and reflectances in the red and near infrared. The means for the red radiances were 12.3 (GSFC) versus 10.1 (UNL) at 52° and 23.0 (GSFC) versus 17.5 (UNL) at 34° . The corresponding means for red reflectance were 4.3 (GSFC) versus 3.9 (UNL) at 52° and 5.9 (GSFC) versus 4.9 (UNL) at 34° . Thus the red measurements determined by GSFC were consistently higher than those acquired by UNL. In contrast, the GSFC's near-infrared radiance means were consistently lower than those determined by UNL: 52.2 (GSFC) versus 54.8 (UNL) at 52° and 62.9 (GSFC) versus 65.2 (UNL) at 34° . The corresponding

near-infrared reflectances were 28.6 (GSFC) versus 31.4 (UNL) at 52° and 25.4 (GSFC) versus 25.9 (UNL) at 34° . However, the overall between team bidirectional reflectance differences were not significant.

The SR (near infrared/red) was 4.3 (GSFC) versus 5.4 (UNL) when computed from radiances at 52° and 2.8 (GSFC) versus 3.7 (UNL) at 34° (see Table 7). When computed from reflectances, the corresponding SRs were higher: 6.7 (GSFC) versus 8.1 (UNL) at 52° and 4.3 (GSFC) versus 5.4 (UNL) at 34° . Whether computed from radiances or reflectances, the SRs determined by UNL were higher than those from GSFC. These results are consistent with LAI measurements taken at the two subsites during the intercomparison field measurement period. These data indicate that UNL sampled a region supporting slightly more dense vegetation (average LAI of 2.1 ± 0.29) than did the GSFC team (LAI of ~ 1.47 ; one sample at central location). Also, θ_s changes may have contributed to these differences. Both teams reported substantial decreases in SR at $\theta = 34^\circ$ compared to the values at 52° , a result consistent with grassland radiance and reflectance responses observed at the FIFE site in 1987 [Middleton, this issue].

Data acquired by the two teams also produced different variances. The % CV in the red region was 75–100% greater for the UNL measurements than for the nadir measurements made by the GSFC team. For example, the CV for red radiance at $\theta_s = 34^\circ$ was 5.5% and 9.6% for the PARABOLA and G-SE590, respectively, but it was 13.0 and 21.9%

for the N-MMR and N-SE590, respectively. This result is most likely related to the greater spatial sampling of the grassland by the UNL team for any θ_s set, which utilized a nearly circular transect approximately 400 m long.

Helicopter versus ground: Each of the ground instrument reflectances were compared with those from the helicopter instruments, although the H-MMR data were only available for the afternoon sample period. The t tests showed differences in some spectral bands for the four ground instruments. The H-MMR reflectances were different from the GSFC team instrument values in the near infrared, although the G-SE590 and H-SE590 were not statistically different for any band. H-MMR and H-SE590 reflectances were different from the UNL team instruments in the blue, green, and red ($\theta = 52^\circ$ only) spectral bands. However, the overall helicopter versus ground differences were not highly significant.

In an attempt to assess the bandwidth and band placement effects on the differences that were observed between the ground and the helicopter instruments, the H-MMR bands were simulated by integrating the high spectral resolution SE590 measurements for each of the three teams, including the H-SE590. These simulated reflectances are given in Table 5b, along with the comparable simulations for the other three types of instruments used in the experiment. Figure 6a presents the H-MMR simulated reflectances (from SE590 instruments) compared with the actual H-MMR, PARABOLA, and N-MMR measurements. If the spectral bandwidths and band placements were the primary cause of reflectance differences between the H-MMR and the other instruments, then the bars of the graph for G-SE590, N-SE590, H-SE590, and H-MMR would all be equal in length (assuming that the spectral band integration/simulations were performed correctly). The results presented in Figure 6a indicate that this is not the case. The large standard deviation for the H-MMR data set also suggests the difficulty in obtaining statistical differences for these data. On the other hand, the graph shows that the differences are small.

ASAS versus ground: Atmospherically corrected ASAS aircraft system surface reflectances in blue, green, red, and near-infrared spectral bands, which could be compared for one time period ($\theta = 52^\circ$), were similar to the ground measurements but were higher by $\sim 1\%$ (versus GSFC) to $\sim 4.5\%$ (versus UNL) in absolute reflectance in the red spectral band. In the near-infrared band the differences were greater at $\sim 4.5\%$ versus GSFC but less than 2% versus UNL in absolute reflectance (see Table 4a). Statistical tests of significance showed that the ground and ASAS reflectances were different in all comparisons except the near-infrared band and the N-MMR blue spectral band.

In the same manner that SE590 simulations were performed for the H-MMR, Table 4b and Figure 6b present the ASAS band reflectance simulations. In addition, since the H-MMR data were not available for the $\theta = 52^\circ$ sample period, the H-MMR was also simulated using the H-SE590 data (referred to as Hsm-MMR in figures). The ASAS-G (GSFC subsite) reflectances should be equivalent to the G-SE590 simulations of the ASAS, and the ASAS-N (UNL subsite) reflectances should be equivalent to the N-SE590 simulations. Accounting for bandwidth and band placement differences appears not to have improved the agreement between the instruments.

Statistical comparisons among similar instruments. The three SE590s (G-SE590, N-SE590, and H-SE590) were compared, and the PARABOLA was compared with MMRs, as they were both designed to have similar spectral band passes analogous to the TM.

SE590s: At a solar zenith angle of 52° the H-SE590 produced the highest reflectance in all four spectral regions (blue, green, red, and near infrared). At $\theta_s = 34^\circ$, however, the H-SE590 produced reflectances intermediate between those measured by the two ground teams for the three visible bands (see Table 5a). Nevertheless, the G-SE590 and the H-SE590 were not significantly different for either solar zenith angle. The N-SE590 and H-SE590 were different in the blue, green, and red band in the morning and in the green band in the afternoon. The G-SE590 and N-SE590 were different in the blue band at both solar zeniths and different in the red band for the morning and green band for the afternoon data sets. These differences may point to the subsite differences for the two teams.

The lack of a significant difference in the G-SE590 versus the H-SE590 reflectances suggest that the helicopter likely sampled a region of site 916 biased toward the GSFC team. This is a real possibility, since the helicopter was attempting to acquire simultaneous spatial/temporal BRDF information with the GSFC team during this time period. At $\theta_s = 34^\circ$ the generally intermediate reflectance determined from the H-SE590 indicates that the helicopter successfully sampled both subsites during the hovering maneuver. However, the simple ratio determined by the H-SE590 was the highest of the three at this Sun angle. The SRs determined by the G-SE590, N-SE590, and H-SE590 were 7.1, 8.8, and 7.0, respectively, at $\theta_s = 52^\circ$ and 4.6, 5.6, and 6.1 at $\theta_s = 34^\circ$. The somewhat higher red reflectance recorded by GSFC, and consequently the lower SR, was probably caused by the placement of the GSFC team on the slightly less dense subsite, a difference that would be emphasized at the lower θ_s of 52° .

MMRs and PARABOLA: The H-MMR and N-MMR can only be compared directly for the $\theta_s = 34^\circ$ data set. Measured values for radiance and reflectance for the H-MMR are higher than the corresponding values acquired by the N-MMR (bands 1–6), but the means are not different owing to the spatial variability captured in these measurements. The CV from the H-MMR was 2.7–9.1 times greater than the CV associated with the N-MMR. Contrarily, the CV for the near infrared associated with the N-MMR was 4.7 times that of the H-MMR.

The PARABOLA and the N-MMR can be compared at both solar zenith angles in three spectral bands (red, near infrared, and shortwave infrared band 2). Although PARABOLA is higher than the H-MMR in the red and the shortwave infrared, the radiances and reflectances are not significantly different, owing to the variability in the H-MMR measurements. The near-infrared measurements for both instruments exhibit relatively smaller variation, but those from the PARABOLA are lower than those measured by the H-MMR. The relatively higher (lower) PARABOLA values in the red (near infrared), translate into lower SRs from the PARABOLA (see Table 7), which is to be expected from the LAI differences and helicopter sampling considerations discussed earlier.

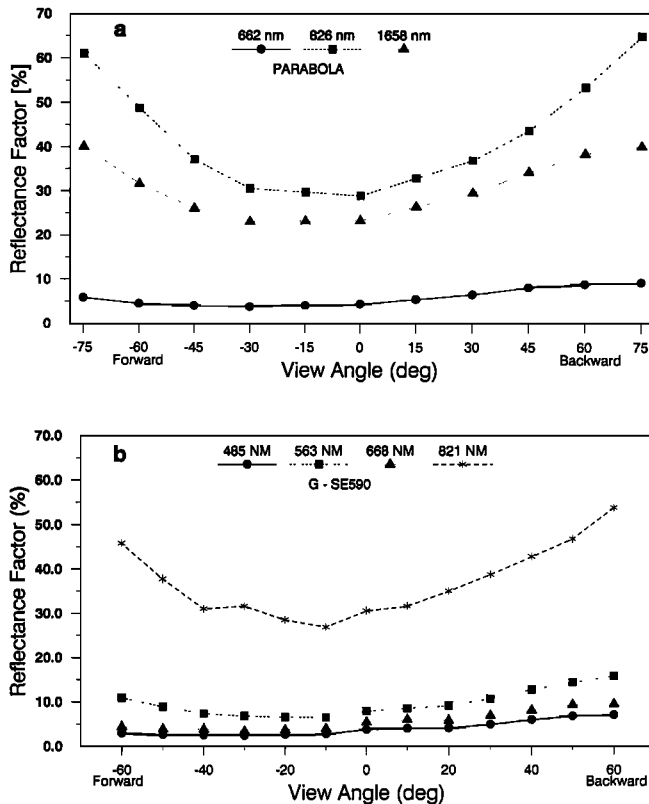


Fig. 7. Bidirectional reflectances for view angles in the solar principal plane at selected wavelengths for a nominal solar zenith angle for the (a) PARABOLA and (b) GSFC SE590 at FIFE site 916, August 8, 1989, $\theta_s = 52^\circ$.

3.3. Instrument Comparisons for Off-Nadir Views

The spectral bidirectional reflectances for the red, near infrared, and shortwave infrared for the nominal $52^\circ \theta_s$ case are presented for the PARABOLA and G-SE590 in Figures 7a and 7b, respectively. These graphs show the typical bowl-shaped vegetation responses described in section 3.1 above, although the broad scaling range deemphasizes the anisotropy. The UNL and helicopter (backscatter off-nadir data only) plots (not shown) were very similar for the comparable spectral wave bands. The importance of this comparison lies in the consistency of view angle feature discrimination by the several instruments in the intercomparison. The SPP bidirectional reflectances for all of the instruments were found to agree rather well qualitatively.

For a more direct comparison the PARABOLA data for the complete diurnal data set (full range of solar zenith angles and viewing angles) was established as a reference for comparisons of the measurements of grassland anisotropy from the several instruments. The complete PARABOLA measurement set (minus the $\theta_s = 52^\circ$ data) was modeled using the general anisotropic model of Ahmad and Deering [this issue]. Then the model output (expected response) for $\theta_s = 52^\circ$ for the red and near-infrared spectral bands was compared with the measurements of the various instruments, as shown in Figure 8.

There was good agreement with the modeled response for all of the instruments in the near-infrared band, although the helicopter and UNL sensor values were generally higher than the modeled or GSFC instrument values, particularly in

the backscatter direction. There was generally good agreement in the red spectral band also, except that the values for the N-SE590 deviate considerably (lower values) from the expected response curve at nadir and in the forward scatter direction. Also, the H-SE590 had a strong outlier (much higher value) at the extreme backscatter angle.

The net effect of the responses in the red and near-infrared spectral bands is represented by the SR and the NDVI for potential biophysical parameter estimations (Figures 8c and 8d, respectively). Although there is reasonably good agreement among the various instruments with the trends for off-nadir angle variations and as compared with the modeled response, the choice of instrument could yield substantially different parameter estimates. The UNL values were consistently higher than the modeled response, while the helicopter values were almost as consistently lower than the modeled value, and by a substantial amount at some viewing angles. The model curve for both ratio indices somewhat overestimates the GSFC instrument values in the backscatter direction.

It is important to note that the SR and NDVI have a marked view angle dependence. Ideally, these indices would have a "flat" response to view angle changes, but all of the instruments show that this is not the case for the prairie grassland. It is important therefore to consider the sensor viewing angle when deriving parameter estimates from such spectral indices.

4. CONCLUSIONS

There are many potential sources of variance for instrument bidirectional reflectance measurement differences. These include measurement errors associated with hardware systems or human operations of the instruments, natural variations that have scaling dependencies, and spectral wave band interval differences. Nevertheless, the bidirectional reflectances from all of the instruments compared were found to agree very well qualitatively and to capture the key spectral effects. They also agreed reasonably well quantitatively, but consistent biases were observed for different instruments or instrument teams. One factor that could account for some of the discrepancies was the variation in the vegetation characteristics between team-specific subsites (GSFC versus UNL) in spite of the attempts to select a uniform area. Different sampling methodologies did not appear to contribute to measured reflectance differences, because every effort was made to minimize these effects through site selection and statistical sample replication.

Solar zenith angle differences must be considered in data intercomparisons. Some of the problems of agreement with the various instrument data most likely resulted from changes in the solar zenith angle during the period of sampling. The magnitude of the solar zenith angle effects were found to be substantial for the two view angles considered.

A wide variation in spectral vegetation index values, computed from radiances and reflectances and from measurements by the various instruments and for different solar zenith angles and sensor viewing angles, points to the need for caution in applying the indices to biophysical parameter assessments. Certainly, further study is warranted to understand these phenomena and to develop algorithms to take advantage of the solar and view angle dependencies or otherwise account for these effects.

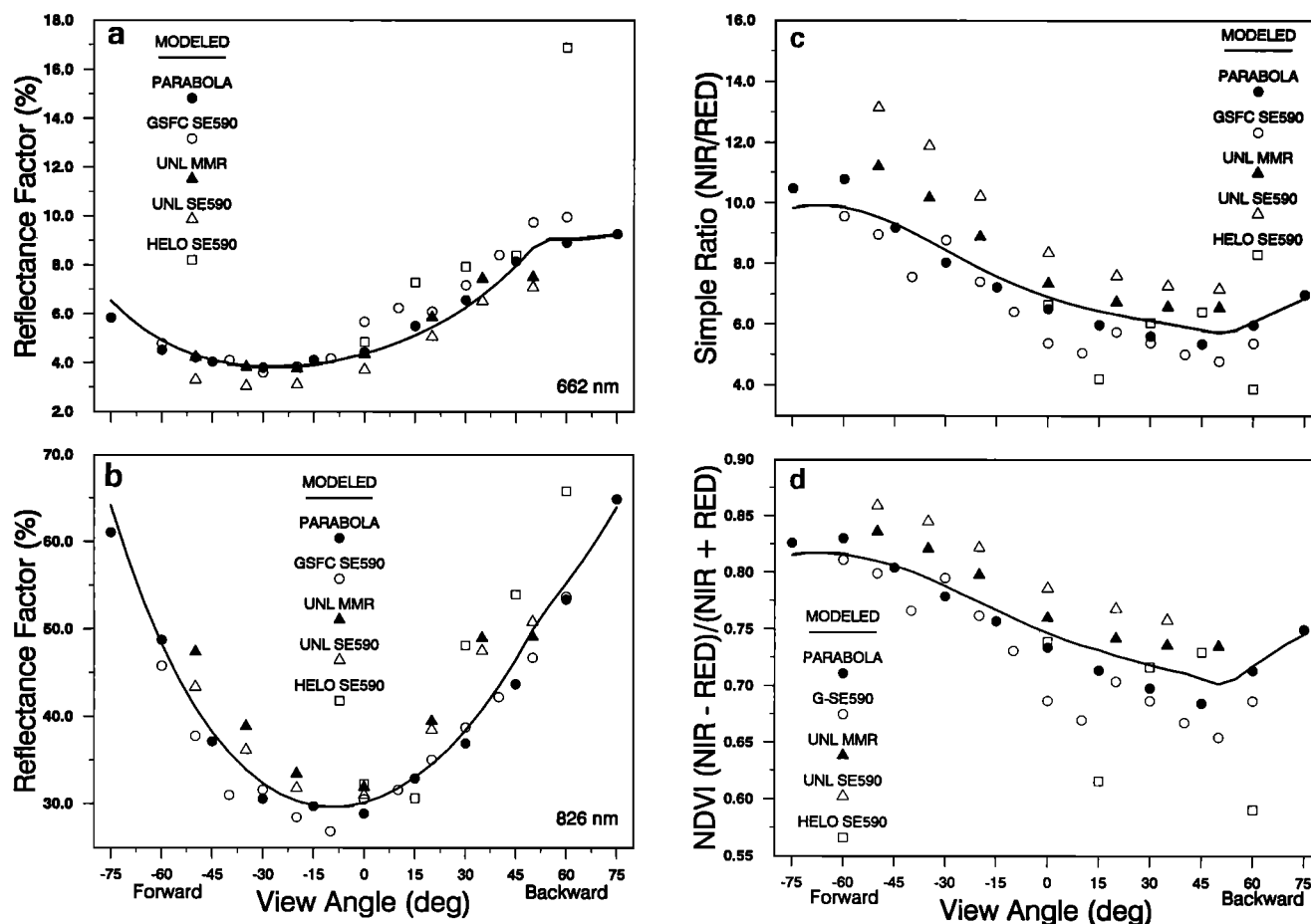


Fig. 8. Nadir and off-nadir solar principal plane reflectances for five instruments compared with modeled PARABOLA values computed from a diurnal series. Comparisons are given for the (a) red, (b) near infrared, (c) simple (NIR/RED) ratio, and (d) NDVI.

There are many potential sources of variation that hinder the development of accurate and robust remote sensing biophysical parameter derivation techniques. This study shows that the general, first-order effects can be successfully captured with a variety of instruments. More subtle features may require high accuracy and precision for feature extraction. Otherwise, they may be lost in the noise of the natural and man-induced variations observed in this evaluation of instruments and approaches to acquiring nadir surface radiances and reflectances.

Acknowledgments. The authors gratefully acknowledge Kansas State University's Evapotranspiration Laboratory personnel, for their superb assistance in all aspects of the ground and air data acquisition campaigns, the Nature Conservancy, for allowing this research to be conducted on the Konza Prairie, and the Kansas Flint Hills ranchers, who enabled access to the off-Konza Prairie sites used in the experiment. The Konza Prairie Research Natural Area is owned by the Nature Conservancy and is operated by the Division of Biology at Kansas State University. This research was supported by NASA Headquarters, Code SE, Washington, D. C., under various RTOPS and university grants.

REFERENCES

- Ahmad, S. P., and D. W. Deering, A simple analytical function for bidirectional reflectance, *J. Geophys. Res.*, this issue.
- Ahmad, S. P., E. M. Middleton, and D. W. Deering, Computation of diffuse sky flux from multidirectional radiance measurements, *Remote Sens. Environ.*, 21, 185–200, 1987.
- Blad, B. L., E. A. Walter-Shea, P. J. Starks, R. C. Vining, C. J. Hays, and M. A. Mesarch, Measuring and modeling near-surface reflected and emitted radiation fluxes at the FIFE site, final report, *Agric. Meteorol. Prog.* 90-1, 159 pp., NASA grant NAG5-894, 1990.
- Deering, D. W., Field measurements of bidirectional reflectance, in *Theory and Applications of Optical Remote Sensing*, pp. 14–65, John Wiley, New York, 1989.
- Deering, D. W., and P. Leone, A sphere-scanning radiometer for rapid directional measurements of sky and ground radiance, *Remote Sens. Environ.*, 19, 1–24, 1986.
- Deering, D. W., and E. M. Middleton, Spectral bidirectional reflectance and effects on vegetation indices for a prairie grassland, in *Proceedings of the Symposium on FIFE, First ISLSCP Field Experiment*, pp. 71–76, American Meteorological Society, Boston, Mass., 1990.
- Deering, D. W., T. F. Eck, and J. Otterman, Bidirectional reflectances of three desert surfaces and their characterization through model inversion, *J. Agric. For. Meteorol.*, 52, 71–93, 1990.
- Flittner, D. E., and P. N. Slater, Stability of narrow-band filter radiometers in the solar-reflective range, *Photogramm. Eng. Remote Sens.*, 57(2), 165–171, 1991.
- Guenther, B., Practical aspects of achieving accurate radiometric field measurements, *Remote Sens. Environ.*, 22, 131–143, 1987.
- Hall, F. G., P. J. Sellers, D. E. Strebel, E. T. Kanemasu, R. D. Kelly, B. L. Blad, B. J. Markham, J. R. Wang, and F. Huemrich, Satellite remote sensing of surface energy and mass balance: Results from FIFE, *Remote Sens. Environ.*, 35, 187–199, 1991.

- Holm, R. G., R. D. Jackson, B. Yuan, M. S. Moran, P. N. Slater, and S. F. Biggar, Surface reflectance retrieval from Thematic Mapper data, *Remote Sens. Environ.*, 27, 47–57, 1989.
- Irons, J. R., K. J. Ranson, D. L. Williams, R. R. Irish, and F. G. Huegel, An off-nadir-pointing imaging spectroradiometer for terrestrial ecosystem studies, *IEEE Trans. Geosci. Remote Sens.*, 29, 66–74, 1991.
- Jackson, R. D., M. S. Moran, P. N. Slater, and S. F. Biggar, Field calibration of reference reflectance panels, *Remote Sens. Environ.*, 22, 145–158, 1987.
- Markham, B. L., and S. P. Ahmad, Radiometric properties of the NS001 Thematic Mapper Simulator aircraft multispectral scanner, *Remote Sens. Environ.*, 34, 133–149, 1990.
- Markham, B., F. Wood, and S. P. Ahmad, Radiometric calibration of the reflective bands of NS001-Thematic Mapper Simulator (TMS) and Modular Multispectral Radiometers (MMR), in Recent Advances in Sensors, Radiometry, and Data Processing for Remote Sensing, *Proc. SPIE Int. Soc. Opt. Eng.*, 24, 96–108, 1988.
- McClatchey, R. A., R. W. Fenn, J. E. A. Selby, F. E. Volz, and J. S. Garing, Optical properties of the atmosphere, *Environ. Res. Pap.* 354, *AFCRL-TR-71-0279*, Air Force Cambridge Res. Lab., Bedford, Mass., 1971.
- Middleton, E. M., Quantifying reflectance anisotropy of photosynthetically active radiation in grasslands, *J. Geophys. Res.*, this issue.
- Nicodemus, F. E., J. C. Richmond, J. J. Hsia, I. W. Ginsberg, T. Limperis, Geometrical considerations and nomenclature for reflectance, *Natl. Bur. Stand. Monogr.* 160, U.S. Govt. Print. Off., Washington, D. C., 1977.
- Pinter, P. J., R. D. Jackson, and M. S. Moran, Bidirectional reflectance factors of agricultural targets: A comparison of ground-, aircraft-, and satellite-based observations, *Remote Sens. Environ.*, 32, 215–228, 1990.
- Robinson, B. F., M. E. Bauer, D. P. DeWitt, L. F. Silva, and V. C. Vanderbilt, Multiband radiometer for field research, in Measurements of Optical Radiations, *Proc. SPIE Int. Soc. Opt. Eng.*, 196, 8–15, 1979.
- Robinson, B. F., R. E. Buckley, and J. A. Burgess, Performance evaluation and calibration of a modular multiband radiometer for remote sensing field research, in Contemporary Infrared Standards and Calibration, *Proc. SPIE Int. Soc. Opt. Eng.*, 308, 147–157, 1981.
- Sellers, P. J., and F. G. Hall, *FIFE Experiment Plan*, p. 141 and appendices, internal document 623, NASA Goddard Space Flight Center, Greenbelt, Md., 1987.
- Sellers, P. J., F. G. Hall, D. E. Strebel, E. T. Kanemasu, R. D. Kelly, B. L. Blad, B. J. Markham, and J. R. Wang, Experiment design and operations, in *Proceedings of the Symposium on FIFE, First ISLSCP Field Experiment*, pp. 1–5, American Meteorological Society, Boston, Mass., 1990.
- Sellers, P. J., F. G. Hall, G. Asrar, D. E. Strebel, and R. E. Murphy, An overview of the First International Satellite Land Surface Climatology Project (ISLSCP) Field Experiment (FIFE), *J. Geophys. Res.*, this issue.
- Slater, P. N., Radiometric considerations in remote sensing, *Proc. IEEE*, 73(6), 997–1011, 1985.
- Tanre, D., C. Deroo, P. Duhaut, M. Herman, and J. J. Morcrette, Description of a computer code to simulate the satellite signal in the solar spectrum: The 5S code, *Int. J. Remote Sens.*, 11, 659–668, 1990.
- Walthall, C. L., and E. M. Middleton, Assessing spatial and seasonal variations in grasslands with spectral reflectances from a helicopter platform, *J. Geophys. Res.*, this issue.
- S. P. Ahmad, B. P. Banerjee, and T. F. Eck, Hughes/STX Corporation, 4400 Forbes Boulevard, Lanham, MD 20706.
- B. L. Blad, C. J. Hays, and E. A. Walter-Shea, Department of Agricultural Meteorology, University of Nebraska, Lincoln, NE 68583.
- D. W. Deering, J. R. Irons, and E. M. Middleton, NASA Goddard Space Flight Center, Code 923, Greenbelt, MD 20771.
- C. L. Walthall, Department of Geography, University of Maryland, College Park, MD 20742.

(Received September 4, 1991;
revised September 9, 1992;
accepted September 15, 1992.)